J|A|C|S
ARTICLES
Published on Web 04/25/2003

# Molecular Recognition of α,β-Unsaturated Carbonyl Compounds Using Aluminum Tris(2,6-diphenylphenoxide) (ATPH): Structural and Conformational Analysis of ATPH Complexes and Application to the Selective Vinylogous Aldol Reaction

Susumu Saito,[‡] Takashi Nagahara,[†] Masahito Shiozawa,[†] Masakazu Nakadai,[†] and Hisashi Yamamoto*[,§]

*Contribution from the Graduate School of Engineering and Graduate School of Science and Institute for Advanced Research, Nagoya University, SORST, Japan Science and Technology Corporation (JST), Chikusa, Nagoya 464-8603, Japan, and Department of Chemistry, University of Chicago, 5735 South Ellis Avenue, Chicago, Illinois 60637*

Received April 25, 2002; E-mail: yamamoto@uchicago.edu

***Abstract:*** Various α,β-unsaturated carbonyl compounds were coordinated with aluminum tris(2,6-diphenylphenoxide) (ATPH) to give the corresponding Lewis acid−base complexes in a distinctive coordination fashion (selective coordination). ATPH recognizes carbonyl substrates and subsequently orients itself as it forms a stable complex through selective coordination with the carbonyl oxygen. Selective coordination also confers a conformational preference to each carbonyl compound under the steric and electronic influence of ATPH, which enables the vinylogous aldol reaction of α,β-unsaturated carbonyl compounds to give the corresponding γ-aldol products with different regio- and stereoselectivities.

## Introduction

Molecular recognition of carbonyl compounds by natural or synthetic receptors has been an active area of research in organic, bioorganic, and supramolecular chemistry. Molecular recognition events involve a wide range of interactions between metals and their ligands,[1] which illustrate the versatility and usefulness of host−guest coordination chemistry in the controlled activation of carbonyl compounds (e.g., CO and $CO_2$).[2] Although these electronic interactions have been the central focus of research, the "template effect",[3] by which overall topology of the product is controlled, has been a pivotal steric interplay that warrants attention in the template-promoted synthesis. The search for a "template" also includes the development of supramolecules[4] in conjunction with the application of metal ions in the design and synthesis of macrocyclic ligands.[5] By contrast, the carbonyl recognition systems of enzymes[6] and their mimics[7] utilize multiple hydrogen bonding to form a complex with carbonyl functionalities. Enzymes discriminate among molecules by forming specific complexes between their active sites and

[†] Graduate School of Engineering, Nagoya University.

[‡] Graduate School of Science and Institute for Advanced Research, Nagoya University.

[§] University of Chicago.

(1) (a) Braterman, P. S., Ed. *Reactions of Coordinated Ligands*; Plenum Press: New York & London, 1989; Vols. 1 and 2. (b) Martell, A. E.; Hancock, R. D.; Smith, R. M.; Motekaitis, R. J. *Coord. Chem. Rev.* **1996**, *149*, 311. (c) Sargeson, A. M. *Coord. Chem. Rev.* **1996**, *151*, 89. (d) Reetz, M. T.; Niemeyer, C. M.; Hermes, M.; Goddard, R. *Angew. Chem., Int. Ed. Engl.* **1992**, *31*, 1017. (e) Buckingham, A. D., Legon, A. C., Roberts, S. M., Eds.; *Principles of Molecular Recognition*; Blackie: Glasgow, U.K., 1993. (f) Hancock, R. D.; Martell, A. E. *Supramol. Chem.* **1996**, *6*, 401.

(2) (a) Constable, E. C., Ed. *Metals and Ligand Reactivity*; VCH: Weinheim, 1996; Chapter 3. (b) Collman, J. P. *Inorg. Chem.* **1997**, *36*, 5145. (c) Collman, J. P.; Fu, L. *Acc. Chem. Res.* **1999**, *32*, 455.

(3) Busch, D. H.; Vance, A. L.; Kolchinski, A. G. In *Comprehensive Supramolecular Chemistry*; Atwood, J. L., Davies, J. E. D., Macnicol, D. D., Vögtle, F., Sauvage, J.-P., Hosseini, M. W., Eds.; Elsevier: Oxford, 1996; Vol. 9, p 1.

(4) (a) Hubin, T. J.; Busch, D. H. *Coord. Chem. Rev.*. **2000**, *200*, 5. (b) Zimmerman, S. C.; VanZyl, C. M.; Hamilton, G. S. *J. Am. Chem. Soc.* **1989**, *111*, 1381. (c) Cram, D. J.; Choi, H.-J.; Bryant, J. A.; Knobler, C. B. *J. Am. Chem. Soc.* **1992**, *114*, 7748. (d) Lehn, J.-M. *Angew. Chem., Int. Ed. Engl.* **1988**, *27*, 89. (e) Cram, D. J. *Angew. Chem., Int. Ed. Engl.* **1988**, *27*, 1009. (f) Pederson, C. J. *Angew. Chem., Int. Ed. Engl.* **1988**, *27*, 1021. (g) Schneider, H.-J. *Angew. Chem., Int. Ed. Engl.* **1991**, *30*, 1417. (h) Cram, D. J.; Tanner, M. E.; Thomas, R. *Angew. Chem., Int. Ed. Engl.* **1991**, *30*, 1024. (i) Petti, M. A.; Shepodd, T. J.; Barrans, R. E., Jr.; Dougherty, D. A. *J. Am. Chem. Soc.* **1988**, *110*, 6825. (j) Kawaguchi, Y.; Harada, A. *J. Am. Chem. Soc.* **2000**, *122*, 3797. (k) Hoshino, T.; Miyauchi, M.; Kawaguchi, Y.; Yamaguchi, H.; Harada, A. *J. Am. Chem. Soc.* **2000**, *122*, 9876 and references therein. (l) Canceill, J.; Cesario, M.; Collet, A. *Angew. Chem., Int. Ed. Engl.* **1989**, *28*, 1246. (m) Garel, L.; Dutasta, J.-P.; Collet, A. *Angew. Chem., Int. Ed. Engl.* **1993**, *32*, 1169. (n) Rose, E.; Quelquejeu, M.; Pandian, R. P.; L.-Nawrocka, A.; Vilar, A.; Richart, G.; Collman, J. P.; Wang, Z.; Straumanis, A. *Polyhedron* **2000**, *19*, 581. (o) *Comprehensive Supramolecular Chemistry*; Atwood, J. L., Davies, J. E. D., Macnicol, D. D., Vögtle, F., Eds.; Elsevier: Oxford, 1996; Vol. 2.

(5) (a) Kolchinski, A. G. *Coord. Chem. Rev.* **1998**, *174*, 207. (b) Martell, A. E.; Motekaitis, R. J.; Lu, Q.; Nation, D. A. *Polyhedron* **1999**, *18*, 3203. (c) Burke, S. D.; O'Donnell, C. J.; Porter, W. J.; Song, Y. *J. Am. Chem. Soc.* **1995**, *117*, 12649. (d) Izatt, R. M., Christensen, J. J., Eds. *Synthesis of Macrocycles: The Design of Selective Complexing Agents (Progress in Macrocyclic Chemistry*; John Wiley & Sons: New York, 1987; Vol. 3.

(6) Fessner, W.-D.; Walter, C. In *Bioorganic Chemistry*; Schmidtchen, F. P., Ed.; Springer: Berlin, 1997; p 97.

(7) (a) Rebek, J., Jr. *Angew. Chem., Int. Ed. Engl.* **1990**, *29*, 245. (b) Pieters, R. J.; Huc, I.; Rebek, J., Jr. *Chem.-Eur. J.* **1995**, *1*, 183. (c) Dugas, H., Ed. *Bioorganic Chemistry*, 3rd ed.; Springer: New York, 1996. (d) Rebek, J., Jr. *Acc. Chem. Res.* **1999**, *32*, 278. (e) Zimmerman, S. C.; Wu, W.; Zeng, Z. *J. Am. Chem. Soc.* **1991**, *113*, 196. (f) Zimmerman, S. C.; Kwan, W.-S. *Angew. Chem., Int. Ed. Engl.* **1995**, *34*, 2404. (g) Corbin, P. S.; Zimmerman, S. C. *J. Am. Chem. Soc.* **1998**, *120*, 9710. (h) Corbin, P. S.; Zimmermann, S. C. *J. Am. Chem. Soc.* **2000**, *122*, 3779. (i) Corbin, P. S.; Zimmerman, S. C.; Thiessen, P. A.; Hawryluk, N. A.; Murray, T. J. *J. Am. Chem. Soc.* **2001**, *123*, 10475.



**10.1021/ja0205941 CCC: $25.00** 

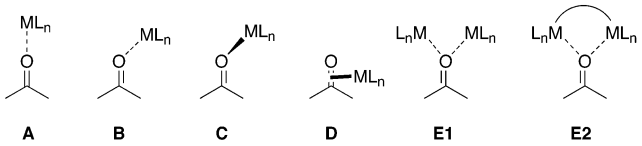


***Figure 1.*** Selective coordination.

substrates, thereby promoting chemical reactivity and selectivity. Unlike these complicated but precise networks extended by weak hydrogen bonding, Lewis acids form characteristic coordination bonds and thus selectively bind substrates using a single metal binding site. Since the appearance of the first report of the formation of crystalline complexes of $BF_3$ and aromatic aldehydes,[8a] Lewis acids have played a prominent role in organic synthesis through their action on carbonyl-containing compounds. They have been used as effective catalysts for a number of C−C bond formations;[9] however, Lewis acid effects, including complementary functions of both the steric and the electronic natures of these acids, still have not been utilized effectively in carbonyl recognition or in selective organic synthesis.[10]

Because carbonyl recognition involves various coordination abilities of Lewis acids, several different modes for coordination of Lewis acids to carbonyl groups, which we call *selective coordination*, will be discussed (Figure 1).[10,11] One is a purely electrostatic interaction, in which the metal is situated at the negative end of the C═O dipole, where C−O−Al = 180° (**A**). The second is the coordination of the metal to one of the lone pairs on the carbonyl oxygen, with the metal lying in the nodal plane of the C═O $\pi$-bond (**B**). This mode of bonding can be seen in a large number of X-ray crystal structures of Lewis acid−base complexes.[8] The third, a bent nonplanar mode of bonding, results from movement of the metal out of the carbonyl $\pi$ nodal plane (**C**). Bulky Lewis acid complexes with esters or amides sometimes prefer this mode.[12] The last mode is $\eta^2$ coordination of a metal to the C═O $\pi$-bond in which the carbonyl $\pi$ orbital is the donor, accompanied by back-bonding into the C═O $\pi^*$ orbital (**D**). Although this mode has been reported for transition metals,[13] it does not seem to occur among main-group elements. Unfortunately, doubly coordinated ter-

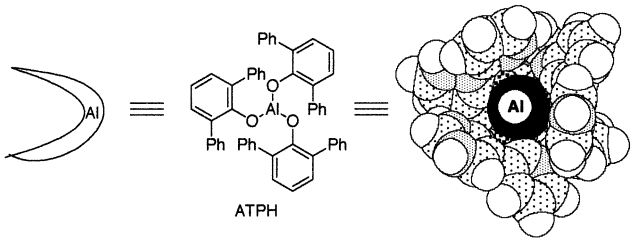


***Figure 2.*** Molecular structure of ATPH.

molecular complexes in mode **E1** are presently unknown. In contrast, Wuest and co-workers recently reported that closely related doubly coordinated bimolecular complexes (**E2**) can be formed when two Lewis acid sites are joined to create single bidentate reagents.[14] The X-ray crystal structure of the bidentate dimercury complex of *N*,*N*-diethylacetamide supports this mode of complexation.[15] Furthermore, Maruoka and Ooi reported that the double coordination of carbonyl compounds by bidentate Lewis acids increases carbonyl reactivity.[16]

We report here that aluminum tris(2,6-diphenylphenoxide) (ATPH)[17] (Figure 2) discriminates among carbonyl substrates through selective coordination of type **B** or **C**, which subsequently causes arrangement of each molecule into a preferred conformation. This observation was unambiguously confirmed by single X-ray crystal structure determination and NMR techniques, and by an in-depth analysis of the structures of ATPH−carbonyl complexes. These data also establish the structures and explain the reactivity of extended dienolates generated by deprotonation of the ATPH−carbonyl complexes, and provide information regarding the origin of the chemo-, regio-, and stereoselective vinylogous aldol reaction[17e] of various α,β-unsaturated carbonyl compounds by use of ATPH.

## Results and Discussions

**Vinylogous Aldol Reaction of α,β-Unsaturated Esters 1 and 4, Aldehydes 3 and 6, and Ketones 2 and 5 Complexed with ATPH.** Sequential treatment of a toluene solution of ATPH (3.3 equiv) with methyl 3-methyl-2-butenoate (**1**) (2.0 equiv) and benzaldehyde (1.0 equiv) at −78 °C was followed by deprotonation with a THF solution of LTMP (2.3 equiv). The reaction mixture was stirred for 30 min and quenched with aqueous $NH_4Cl$ to give homoallyl alcohol **7a** in 91% isolated yield (entry 1, Table 1). The predominant alkylation site was at the (*Z*)-$\gamma$ position of **1** ((*Z*)-$\gamma$:(*E*)-$\gamma$ = 13:1). In sharp contrast, mesityloxide (**2**) and senecialdehyde (**3**) gave the (*E*)-$\gamma$-products

(8) (a) Landolf, C. R. *Hebd. Seances Acad. Sci.* **1878**, *86*, 671. (b) Schreiber, S. L. In *Comprehensive Organic Synthesis*; Trost, B. M., Fleming, I., Eds.; Pergamon Press: Oxford, 1991; Vol. 1, p 283. (c) Shambayashi, S.; Crowe, W. E.; Schreiber, S. L. *Angew. Chem., Int. Ed. Engl.* **1990**, *29*, 256. (d) Denmark, S. E.; Almstead, N. G. *J. Am. Chem. Soc.* **1993**, *115*, 3133. (e) Reetz, M. T.; Hüllmann, M.; Massa, W.; Berger, S.; Rademacher, P.; Heymanns, P. *J. Am. Chem. Soc.* **1986**, *108*, 2405 and references therein. (f) Corey, E. J.; Rohde, J. J.; Fischer, A.; Azimioara, M. D. *Tetrahedron Lett.* **1997**, *38*, 33.

(9) (a) *Lewis Acids in Organic Synthesis*; Yamamoto, H., Ed.; Wiley-VCH: Weinheim, 2000; Vols. 1 and 2. (b) *Lewis Acid Reagents: A Practical Approach*; Yamamoto, H., Ed.; Oxford University Press: Oxford, 1999.

(10) (a) Ooi, T.; Maruoka, K. In *Modern Carbonyl Chemistry*; Otera, J., Ed; Wiley-VCH: Weinheim, 2000; pp 1−32. (b) Saito, S.; Yamamoto, H. In *Modern Carbonyl Chemistry*; Otera, J., Ed; Wiley-VCH: Weinheim, 2000; pp 33−67.

(11) For an excellent review, see: (a) Healy, M. D.; Power, M. B.; Barron, A. R. *Coord. Chem. Rev.* **1994**, *130*, 63. (b) Adams, R. D.; Chen, G.; Chen, L.; Wu, W.; Yin, J. *J. Am. Chem. Soc.* **1991**, *113*, 9406. (c) LePage, T. J.; Wiberg, K. B. *J. Am. Chem. Soc.* **1988**, *110*, 6642.

(12) (a) Parks, D. J.; Piers, W. E. *J. Am. Chem. Soc.* **1996**, *118*, 9440. (b) Power, M. B.; Bott, S. G.; Clark, D. L.; Atwood, J. L.; Barron, A. R. *Organometallics* **1990**, *9*, 3086. (c) Quinkert, G.; Becker, H.; Grosso, M. D.; Dambacher, G.; Bates, J. W.; Dürnere, G. *Tetrahedron Lett.* **1993**, *34*, 6885. (d) Shreve, A. P.; Mulhaupt, R.; Fultz, W.; Calabrese, J.; Robbins, W.; Ittel, S. D. *Organometallics* **1988**, *7*, 409. (e) Healy, M. D.; Mason, M. R.; Barron, A. R.; Gravelle, P. W.; Bott, S. G. *J. Chem. Soc., Dalton Trans.* **1993**, 441. See also ref 10.

(13) For a review, see: (a) Gladysz, J. A.; Boone, B. J. *Angew. Chem., Int. Ed. Engl.* **1997**, *36*, 550. (b) Lenges, C. P.; Brookhart, M.; White, P. S. *Angew. Chem., Int. Ed.* **1999**, *38*, 552.

(14) For reviews, see: (a) Wuest, J. D. *Acc. Chem. Res.* **1999**, *32*, 81. (b) Vaugenois, J.; Simard, M.; Wuest, J. D. *Coord. Chem. Rev.* **1995**, *145*, 55. The bidentate mode involving two aluminum centers, see: (c) Sgarma, V.; Simard, M.; Wuest, J. D. *J. Am. Chem. Soc.* **1992**, *114*, 7931. See also ref 11b.

(15) Vaugeois, J.; Wuest, J. D. *J. Am. Chem. Soc.* **1998**, *120*, 13016.

(16) Ooi, T.; Takahashi, M.; Maruoka, K. *J. Am. Chem. Soc.* **1996**, *118*, 11307. See also ref 10a.

(17) For a preliminary communication and related works for the present article, see: (a) Saito, S.; Shiozawa, M.; Nagahara, T.; Nakadai, M.; Yamamoto, H. *J. Am. Chem. Soc.* **2000**, *122*, 7847. (b) Saito, S.; Shiozawa, M.; Yamamoto, H. *Angew. Chem., Int. Ed.* **1999**, *38*, 1769. (c) Saito, S.; Ito, M.; Shiozawa, M.; Yamamoto, H. *J. Am. Chem. Soc.* **1998**, *120*, 813. (d) Saito, S.; Yamamoto, H. *Chem.-Eur. J.* **1999**, *5*, 1959. (e) Casiraghi, G.; Zanardi, F.; Battistini, L.; Appendino, G. *Chemtracts* **1999**, 547. Very recent applications of ATPH, see: (f) Saito, S.; Yamazaki, S.; Yamamoto, H. *Angew. Chem., Int. Ed.* **2001**, *40*, 3613. (g) Saito, S.; Sone, T.; Murase, M.; Yamamoto, H. *J. Am. Chem. Soc.* **2000**, *22*, 10216. For a review of ATPH, see: (h) Saito, S.; Yamamoto, H. *Chem. Commun.* **1997**, 1585. (i) Yamamoto, H.; Yanagisawa, A.; Ishihara, K.; Saito, S. *Pure Appl. Chem.* **1998**, *70*, 1507. (j) Yamamoto, H.; Saito, S. *Pure Appl. Chem.* **1999**, 71, 239.

***Table 1.*** Aldolization of α,β-Unsaturated Carbonyl Compounds with Aldehydes Using ATPH[a]

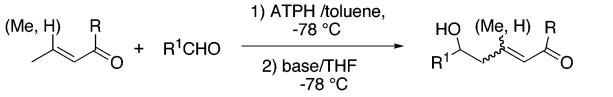


| entry | α,β-unsaturated carbonyl compound | $R^1CHO$ | base | aldol adduct | aldol adduct yield %[b] (*E*:*Z*) |
|---|---|---|---|---|---|
| 1 | 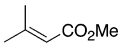 **1** | PhCHO | LTMP | **7a** | 91 (1:13)[c] |
| 2 | | *c*-HexCHO | LTMP | **7b** | 80 (1:14)[c] |
| 3 | 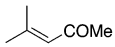 **2** | PhCHO | LDA | **8a** | 84 (>99:1) |
| 4 | | *c*-HexCHO | LDA | **8b** | 65 (>99:1) |
| 5 | 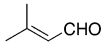 **3** | PhCHO | LDA | **9a** | 99 (>99:1) |
| 6 | | PhCHO | LTMP | **9a** | 99 (>99:1) |
| 7 | | *c*-HexCHO | LDA | **9b** | 81 (>99:1) |
| 8 | 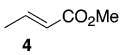 **4** | PhCHO | LTMP | **10** | 97 (>99:1)[c] |
| 9 | 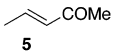 **5** | PhCHO | LDA | **11** | 82 (>99:1) |
| 10 | 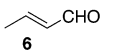 **6** | PhCHO | LDA | **12** | 99 (>99:1) |

[a] Unless otherwise specified, reactions were performed using α,β-unsaturated carbonyl compound (1.0 equiv), $R^1CHO$ (1.0 equiv), base (1.2 equiv), and ATPH (2.2 equiv). [b] Of isolated, purified products. [c] α,β-Unsaturated carbonyl compound (2.0 equiv), base (2.3 equiv), and ATPH (3.3 equiv) were used.

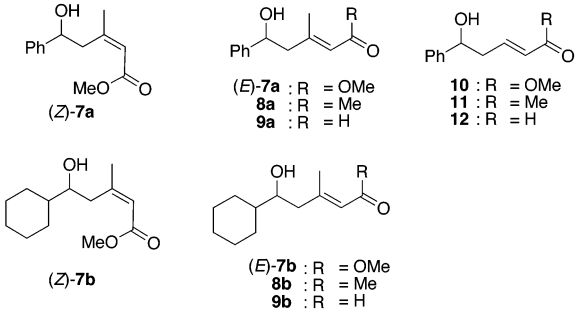


exclusively (entries 3−7). None of the α-alkylated product was obtained in either case. Varying the lithium amide or aldehyde with their derivatives did not affect the *E*:*Z* selectivities (entries 5−7). As compared with the stereochemical reversal observed between β,β-disubstituted-α,β-unsaturated ester **1** and aldehyde **3**, exclusive *E*-selectivity was consistently obtained using β-monosubstituted-α,β-unsaturated ester **4**, ketone **5**, and aldehyde **6** (entries 8−10). However, the α,β-unsaturated amide (*E*)-*N*,*N*-dimethyl-2-butenamide was inert and gave no aldol products under similar reaction conditions (data not shown).

**Comparison of Single-Crystal Structures of ATPH−α,β-Unsaturated Aldehyde, Ester, and Ketone Complexes.** To explain the above results, the X-ray crystal structures of the ATPH complexes of **1**−**3** (Figure 3), **4**, and **6** (Figure 4) were obtained. Particularly notable structural features of these ATPH−carbonyl complexes include the Al−O−C angles and Al−O distances (Table 2), which confirm that the size and shape of the cavity change depending on the substrate. The angle values $\theta$ and $\phi$[8b,12] shed light on the coordination mode of the carbonyls, and results obtained from the X-ray crystal structures of ATPH−carbonyl complexes are worthy of comment. With the exception of the coordination of metals that slightly deviate from the $\pi$ nodal plane (i.e., mode **B** with $\phi < 5°$), the $\phi$ values show that the carbonyl is instead coordinated with the metal in mode **C**. The $\theta$ values vary with different carbonyl substrates (i.e., the coordination seems inherent to each substrate). Apparently, the selective coordination of carbonyls to bulky ATPH, indicated by both the $\phi$ and the $\theta$ values, is quite flexible, and steric effects predominate. However, some general rules have been derived from a series of these distinctive $\theta$ values, which govern the formation of ATPH−carbonyl complexes. All five ATPH complexes adopt an *s-trans* conformation with respect to the (O═C)−(C═C) single bond axis,[18] although each carbonyl substrate (shown in light blue) obviously has a different coordination pattern. Whereas aldehydes **3** and **6** with Al−O═C angles ($\theta$) of 193.9(4)° and 214.1(3)°, respectively, favor *anti*-complexation ($\theta > 180°$), esters **1** and **4** and ketone **2** with $\theta$ = 136.2(3)°, 143.2(3)°, and 148.2(2)°, respectively, show *syn*-complexation ($\theta < 180°$) (Table 2).[19] Thus, aldehydes **3** and **6** prefer *anti*, *s-trans* conformation, while methyl esters **1** and **4** and ketone **2** prefer *syn*, *s-trans* conformations in complexes with ATPH. These results are in accord with the coordination bias of conjugated carbonyl compounds with relatively small Lewis acids.[8] Given the preferential conformation, each *Z* and *E* γ-methyl group of these three substrates is affected by a distinct steric environment. The (*Z*)-γ-methyl of **1** and the (*E*)-γ-methyl of **3** occupy sterically less hindered space, that is, relatively outside of the cavity of ATPH (Figures 2 and 3). Initially, it is rather difficult to discriminate the different steric effects acting on the two γ-methyl groups of the ketone complex. In practice, the equivocal location of these γ-methyl groups leads to aldolization with product diversity, which will be discussed later in this paper. It also should be pointed out that the methyl group of the methoxy group of esters **1** and **4** adopts the *trans* (or *Z*) conformation with respect to the carbonyl,[20] being arranged around the C−O single bond axis. This is consistent

(18) For the general aspects of the conformation (*s-cis* vs *s-trans*) of unsaturated carbonyl compounds, see: *Stereochemistry of Organic Compounds*; Eliel, E. L., Wilen, S. H., Eds.; John Wiley & Sons: New York, 1994; Chapter 10.2., pp 615 and 622. Also see the depiction below for two major conformations of an α,β-unsaturated carbonyl compound and diene, respectively. The definition for the conformations (*s-trans* and *s-cis*, where "*s*" denotes a "single bond") of an extended dienolate is based on that for a diene.


(19) For a discussion of the coordination aptitude of a variety of Lewis acids toward carbonyl compounds (e.g., *syn*- vs *anti*-coordination), see refs 8b and 8c. See below for the general definition of *syn*- and *anti*-complexations of α,β-unsaturated carbonyl compounds, which denotes the complexation mode of the Lewis acid ($ML_n$) with respect to the orientation of the α,β-double bond.

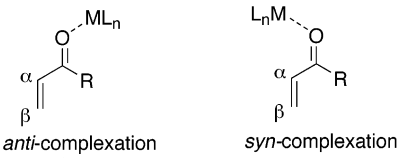


(20) For the definition of the trans (or *Z*) or cis (or *E*) orientation of the alkoxy group of ester functionality, see: *Stereochemistry of Organic Compounds*; Eliel, E. L., Wilen, S. H., Eds.; John Wiley & Sons: New York, 1994; Chapter 10.2., p 618. See also below for the definition.

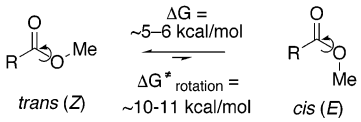

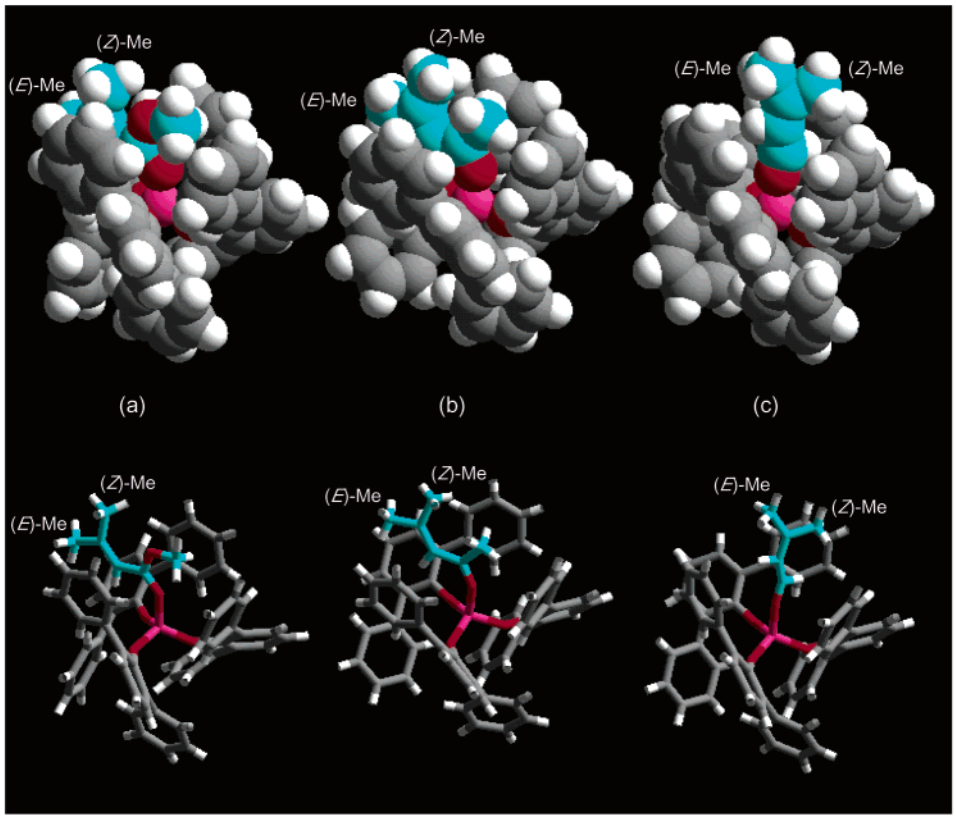


***Figure 3.*** The X-ray crystal structures (CPK (upper) and cylinder (lower) models) of (a) ATPH−**1**, (b) ATPH−**2**, and (c) ATPH−**3** complexes. Light blue color denotes carbonyl compounds.

with the general preference for the *trans* orientation of the methyl and ethyl groups of the alkoxy groups of free esters.[20]

**Comparison of $^1$H NMR Spectra of ATPH−α,β-Unsaturated Aldehyde, Ester, and Ketone Complexes.** To further confirm the differing steric effects exerted by ATPH on each carbonyl substrate in solution, we measured $^1$H NMR shift changes ($\Delta\delta$) from free to bound substrates.[21] $^1$H NMR spectra of the ATPH−**6** complex (300 MHz, $CD_2Cl_2$ or toluene-$d_8$) revealed that the original chemical shifts of the aldehydic proton ($H_a$) at $\delta$ 9.50, and the α- and β-carbon protons ($H_b$ and $H_c$) at $\delta$ 6.13 and $\delta$ 6.89, respectively, were shifted significantly upfield to $\delta$ 6.21, $\delta$ 4.92, and $\delta$ 6.40, respectively. The largest $\Delta\delta$ value of $H_a$ of 3.29 ppm suggests that the carbonyl is effectively shielded by the arene rings of the cavity. This observation is in contrast to the resonance frequencies of the $Et_2AlCl$−**6** complex at −60 °C ($H_a$, $\delta$ 9.32; $H_b$, $\delta$ 6.65; $H_c$, $\delta$ 7.84) and those of complexes of **6** with other ordinary Lewis acids.[22] Other examples are listed in Table 3. In general, similar upfield shifts are also seen in other ATPH−carbonyl complexes. More significant upfield shift changes were observed with the (*E*)-γ-methyl of **1** and the (*Z*)-γ-methyl of **3**, as compared with the (*Z*)-γ-methyl of **1** and the (*E*)-γ-methyl of **3**, respectively. This indicates that the former two methyl groups are more magnetically, and hence more sterically, shielded by the phenyl rings of ATPH. In contrast, the two γ-methyl groups of the ATPH complex of ketone **2** showed an upfield shift of similar magnitude. The ester complexes of **1** and **4**, slightly different in structure, showed similar shift changes. These $^1$H NMR experiments performed in organic solvent are entirely consistent with the data obtained by the single-crystal X-ray analyses. The data indicated that the cavity of ATPH can differentiate among carbonyl substrates that, once accepted into the cavity, exhibit unprecedented reactivity and selectivity under the steric and electronic environment of the arene rings.

**$^1$H NMR Studies of Extended Enolate Intermediates of an Aldehyde, Ester, and Ketone Complexed with ATPH.** Upon deprotonation of the ATPH−carbonyl complexes, extended dienolates bound to ATPH result. To confirm the characteristics and structural nature of the extended dienolates, low temperature $^1$H NMR and nOe measurements were carried out. We observed nOe (NOEDIF; toluene-$d_8$−THF-$d_8$, −78 °C) enhancement between $H_a$ and $H_d$ of the ATPH-dienolate of **3**, but negligible nOe between $H_a$ and $H_c$ (Figure 5). Furthermore, the $^1$H−$^1$H coupling constant (12.2 Hz) and lack of nOe enhancement between $H_a$ and $H_b$ indicate that these two protons are in an *E* relation. These data support $\mathbf{I_1}$ as the most preferred structure [$^1$H NMR: $\delta$ 4.73 (d, 1H, $J$ = 12.3 Hz, $H_a$), 4.21 (s, 1H, C=$H_c$H$_c$), 4.25 (d, 1H, $J$ = 12.4 Hz, $H_b$), 4.12 (s, 1H, C=H$_c$$H_c$), 1.31 (s, 3H, C($H_d$)$_3$) ppm] and provide evidence that the *s-trans* conformer of the ATPH−**3** complex was translated into the *E*, *s-trans* dienolate conformer $\mathbf{I_1}$, rather than $\mathbf{I_2}$−$\mathbf{I_4}$ (Figure 5). This also means that the ATPH−**3** complex and the corresponding extended dienolate $\mathbf{I_1}$ have similar structures.

In contrast, the nOe spectrum gave coupling constants of similar magnitude between $H_b$ and $H_c$ as well as $H_b$ and $H_d$ ($\delta$ 1.29 ppm) for the ester dienolate (Figure 6), suggesting that the $H_b$ peak has an average shift between $\mathbf{I_5}$ and $\mathbf{I_6}$. A set of three broadened singlet peaks of 2$H_c$ ($\delta$ 4.08 and 3.88 ppm)

(21) We always observed $^1$H NMR shifts exactly corresponding to 1:1 complexes between ATPH and carbonyl compounds. A slow exchange between free and bound substrates on a NMR time scale caused neither shifts of free carbonyl compounds nor average shifts between these substrates.
(22) Childs, R. F.; Mulholland, D. L.; Nixon, A. *Can. J. Chem.* **1982**, *60*, 801.

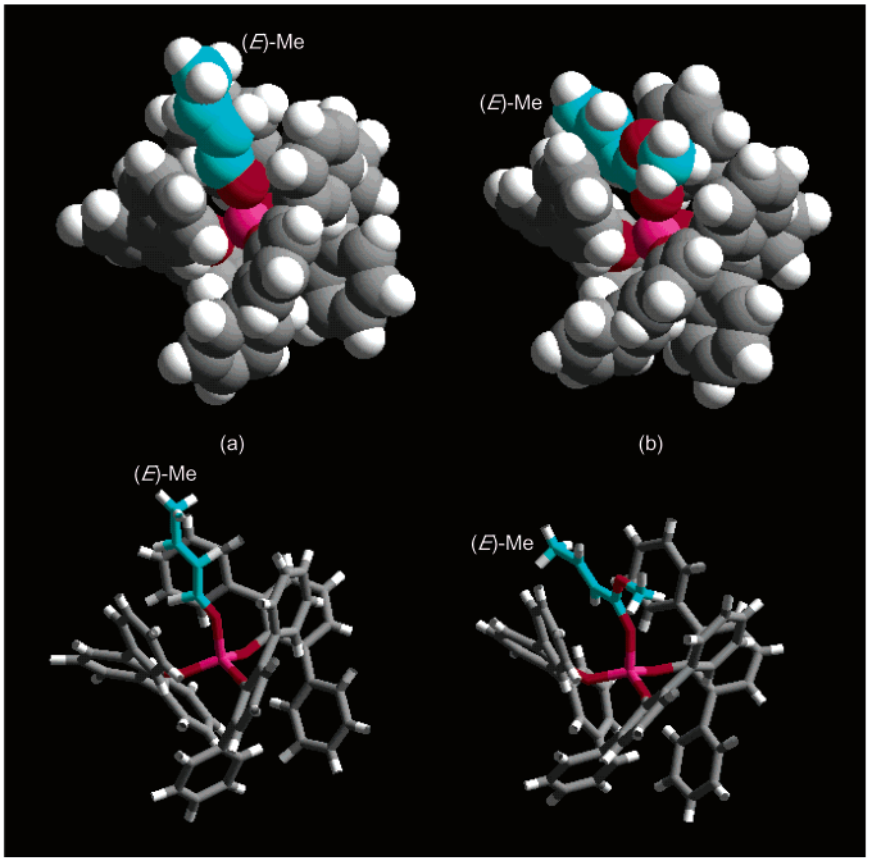


***Figure 4.*** The X-ray crystal structures (CPK (upper) and cylinder (lower) models) of (a) ATPH−**6**, (b) ATPH−**4** complexes. Light blue color denotes carbonyl compounds.

***Table 2.*** Selected Metrical Data for ATPH−Carbonyl Complexes

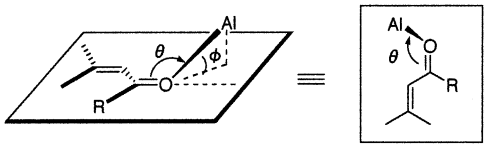


| property | ATPH–**1** (R = OMe) | ATPH–**2** (R = OMe) | ATPH–**3** (R = H) | ATPH–**4** (R = OMe) | ATPH–**6** (R = H) |
|---|---|---|---|---|---|
| C═O, Å | 1.249(5) | 1.262(3) | 1.128(6) | 1.30(1) | 1.152(5) |
| Al−O ($sp^2$), Å | 1.833(3) | 1.823(2) | 1.810(3) | 1.803 | 1.829(2) |
| $\theta$, ° | 136.2(3) | 148.1(2) | 193.9(4) | 143.1(3) | 214.1(3) |
| $\phi$, ° | 4.2 | 13.5 | 16.9 | 19.9 | 6.1 |
| other Al−O−C angles | 132.5(3) 152.4(4) 159.2(3) | 130.7(2) 150.0(2) 151.8(2) | 137.3(3) 142.3(3) 145.0(3) | 133.0(1) 142.7(4) 148.9(4) | 136.7(2) 145.0(2) 150.8(2) |

and $H_b$ ($\delta$ 2.58 ppm) also supports a fast equilibrium between $\mathbf{I_5}$ and $\mathbf{I_6}$ on the NMR time scale. The dienolate of ketone **2** showed two sets of broadened peaks corresponding to $H_b$, $H_c$, and $H_d$ at −20 °C [six peaks: first set, $\delta$ 4.28 (bd, $J$ = 3.6 Hz, 2/5H), 4.01 (bs, 2/5H), 3.99 (bs, 2/5H) ppm; second set, $\delta$ 4.21 (b, 3/5H), 3.96 (bd, $J$ = 3.6 Hz, 3/5H), 3.74 (s, 3/5H) ppm], suggesting that the equilibria are more complicated and involve more than two conformers of the dienolate. At −78 °C, four broad peaks appeared in the region of 4.30−3.58 ppm, which certainly involves $H_b$, $H_c$, and $H_d$. These peaks are not discernible, but are split into six peaks, rather sharpened but with some broadening, upon warming to −20 °C. Decoupling experiments with these peaks, whose chemical shift regions were approximately the same, were not helpful. Further warming of the sample or allowing the sample to settle for an hour at −20 °C resulted in decomposition of the dienolate. Thus, unequivocal identification of the structure of every conformer was not possible and was obtained only with the aldehyde and ester.

***Table 3.*** $^1$H NMR Chemical Shift Changes ($\delta_{bound} - \delta_{free} = \Delta\delta$) from Free (**1**−**4**) to Bound (ATPH−**1**−**4**) Substrates

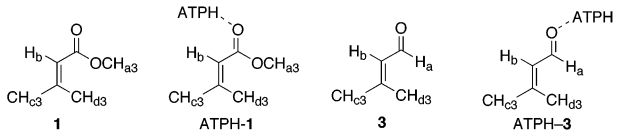


| compound | chemical shift (ppm) $H_a$ | $H_b$ | $H_c$ ($E$) | $H_d$ ($Z$) | compound | chemical shift (ppm) $H_a$ | $H_b$ | $H_c$ ($E$) | $H_d$ ($Z$) |
|---|---|---|---|---|---|---|---|---|---|
| **1**, $\delta_{free}$ | 3.68 | 5.69 | 2.17 | 1.90 | **3**, $\delta_{free}$ | 9.96 | 5.88 | 1.99 | 2.18 |
| ATPH–**1**, $\delta_{bound}$ | 2.17 | 4.53 | 0.93 | 1.25 | ATPH–**3**, $\delta_{bound}$ | 6.74 | 4.54 | 1.24 | 1.05 |
| $\Delta\delta$ | -1.51 | -1.16 | -1.24 | -0.65 | $\Delta\delta$ | -3.22 | -1.34 | -0.75 | -1.13 |

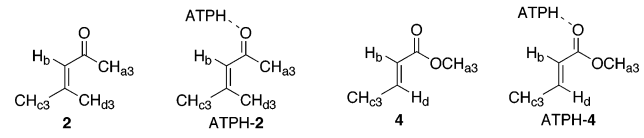


| compound | chemical shift (ppm) $H_a$ | $H_b$ | $H_c$ ($E$) | $H_d$ ($Z$) | compound | chemical shift (ppm) $H_a$ | $H_b$ | $H_c$ ($E$) | $H_d$ ($Z$) |
|---|---|---|---|---|---|---|---|---|---|
| **2**, $\delta_{free}$ | 2.01 | 5.65 | 1.78 | 1.42 | **4**, $\delta_{free}$ | 3.37 | 5.66 | 1.30 | 6.78 |
| ATPH–**2**, $\delta_{bound}$ | 0.67 | 4.67 | 1.11 | 0.94 | ATPH–**4**, $\delta_{bound}$ | 2.17 | 4.49 | 0.81 | 5.83 |
| $\Delta\delta$ | -1.34 | -0.98 | -0.67 | -0.48 | $\Delta\delta$ | -1.20 | -1.17 | -0.95 | -0.49 |

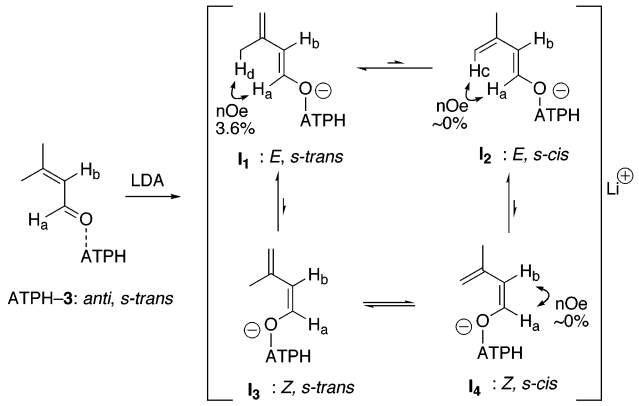


***Figure 5.*** The structural relationship between the conformers of **3** and the corresponding extended dienolate.

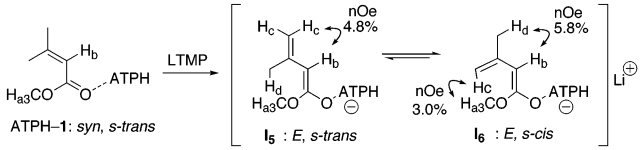


***Figure 6.*** Equilibrium between the most important *s-trans* and *s-cis* conformations of ester dienolate.

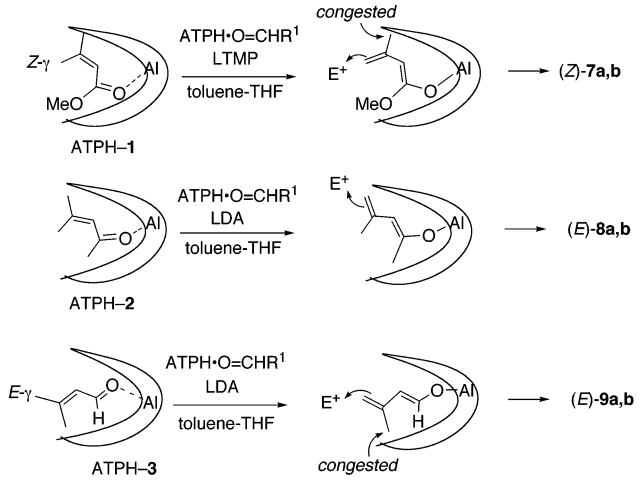


***Figure 7.*** Illustrative depictions of ATPH−**1**, ATPH−**2**, and ATPH−**3** complexes and their dienolate intermediates as more reactive conformers. $E^+$ denotes ATPH·O=CHR[1] or R[1]CHO, or other reactive species.[24]

This also implies that the ensuing aldolization has potential to yield a complex mixture of products.

With these data in hand, simple models of the ATPH complexes of the three carbonyl substrates **1**−**3** and the corresponding dienolates are illustrated (Figure 7). We can see *anti*-complexation, although approximately linear, with the aldehyde, and *syn*-complexation with the ketone and the ester. These two *syn*-complexes are distinct from each other, with the ester having a C−O−Al angle ($\theta$) of 136°, which is less than that of the ketone complex ($\theta = 148.1°$). If we assume that the structure of the resulting extended dienolate resembles the corresponding ATPH−carbonyl complex, the different selectivity can be explained by the distinctive selective coordination of each substrate. Because the *s-cis*−*s-trans* equilibrium of the extended dienolate of ester **1** is very rapid, it may conform to Curtin−Hammet kinetic control, which requires us to consider the more reactive conformation toward an electrophile in the transition state ensemble. It is reasonable to suggest that the

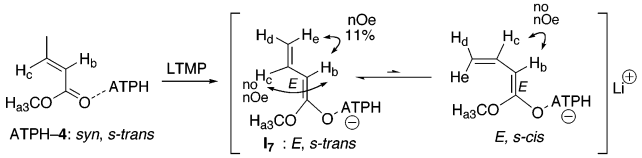


***Figure 8.*** Of greatest importance is the *s-trans* dienolate conformer $\mathbf{I_7}$.

*s-cis* conformer $\mathbf{I_6}$ is a more reactive form than the *s-trans* conformer $\mathbf{I_5}$ in a rapid equilibrium, the former being altered for addition due to steric reasons.[23] In contrast, the *s-trans* conformer of the aldehyde dienolate $\mathbf{I_1}$ is the only species that was observable and should be more reactive. Apparently the terminal methylene group of the *s-trans* form $\mathbf{I_1}$ is sterically less shielded by ATPH than that of the *s-cis* form $\mathbf{I_2}$ when an electrophile approaches from outside the cavity (Figures 3 and 7). The difference between these two cases is easily discernible. However, the predominant *E*-selectivity with the ketone dienolate is not easily explained because the two $\gamma$-methyl groups are under similar steric influences and the dienolate involves several conformers. Other possible mechanisms[24] cannot be ruled out, and the NMR results only suggest that the preponderance of the *s-trans* conformer contributes to the exclusive *E*-selectivity.

**Rational Explanation for the Consistent *E*-Selectivity Observed with β-Monosubstituted-α,β-unsaturated Carbonyl Compounds 4−6.** As mentioned earlier, the *E*/*Z* selectivity reversal was observed between the reactions of $\beta$-mono- and $\beta,\beta$-disubstituted esters **1** and **4** (entries 1 and 8, Table 1). This also can be rationalized by similar NMR experiments of the dienolate of the ATPH−**4** complex (Figure 8). Chemical shifts of the four vinylic protons provided significant information that corroborated the structure of the dienolate. These peaks are in accordance with $H_b$ [$\delta$ 2.79 (d, $J = 11.1$ Hz)], $H_c$ [$\delta$ 6.03 (ddd, $J = 11.1, 12.1, 18.0$ Hz)], $H_d$ [$\delta$ 3.66 (d, $J = 12.0$ Hz)], and $H_e$ [$\delta$ 3.76 (d, $J = 18.0$ Hz)], which appeared immediately upon deprotonation at −78 °C.

The coupling constant of $H_c-H_e$ (18.0 Hz), being larger than that of $H_c-H_d$ (12.0 Hz), favors $H_c$ and $H_e$ in an *E* relationship. Upon irradiation of $H_b$, nOe enhancement was observed with $H_e$ but not with $H_c$, suggesting that the dienolate adopted the *s-trans* conformation. The dihedral angle of (H$_2$C=C)−(C=C−O) should be very close to 180° on the basis of the Karplus rule[25] because the coupling constant of $H_b-H_c$ (11.1 Hz) is greater than 10 Hz. Thus, the structure of **4** bound to ATPH was maintained into the resulting dienolate. Consequently, *E*-product **10** should be formed through this more stable *s-trans* conformer $\mathbf{I_7}$ (Figures 8 and 9), in contrast to the fast equilibrium involving the dienolate of **1**, which prefers the reaction of *s-cis* conformer $\mathbf{I_6}$.

In this context, ATPH had less steric influence on the electrophile that attacked the dienolate, because the structure of the dienolate with a negligible amount of *s-cis* conformer

(23) In fact, a rapid equilibrium (*s-trans* ⇄ *s-cis*, for example, see Figure 6) faster than the rate of aldolization is envisioned by complete reversal of the olefin configuration (the *E*-$\gamma$-methyl of (*Z*)-**15** was delivered to the *Z*-$\gamma$-methylene of **20**).

(24) As one of the referees suggested, significant effects of the second equivalent of ATPH, which presumably activates the aldehyde partner, need further investigation. In the absence of the second ATPH, a considerable decrease in chemical yields was consistently observed.

(25) (a) Karplus, M. *J. Chem. Phys.* **1959**, *30*, 11. (b) *Application of NMR Spectroscopy in Organic Chemistry*, 2nd ed.; Jackman, L. M., Sterhell, S., Eds.; Pergamon Press: New York, 1969.

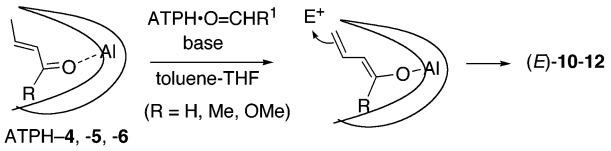


***Figure 9.*** Comparable reactivities of ATPH−**4**, −**5**, −**6** complexes to give *E*-products. Selective coordination is not important.

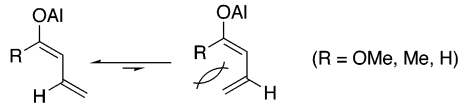


***Figure 10.*** Preponderance of the *s-trans* conformer.

directly reflected the product distributions irrespective of the R groups, that is, the mode of the selective coordination (Figure 9). Absolute *E*-selectivity derived from **5** and **6** could be explained by a similar argument, considering the general nature favoring the *s-trans* conformer in dienolates of this type (Figure 10).[26]

**Vinylogous Aldol Reaction of α,*β*-Unsaturated Aldehyde 13, Ester 15, and Ketone 14 Complexed with ATPH.** By taking advantage of the distinct recognition ability of ATPH toward carbonyl compounds, we next examined the regio- and stereoselectivity of substrates **13**−**15**, which have different substituents at the $\beta$-positions. The reaction profiles obtained are very striking (Scheme 1). The *E*-aldehyde was deprotonated and subsequently alkylated regioselectively at the $\gamma$-*E*-position to give the *E*-product **16**. In comparison, the deprotonation proceeded chemoselectively ($\gamma$-methyl vs $\gamma$-methylene) at the $\gamma$-methyl group of *E*-ester **15**, and the rapid *s-cis*−*s-trans* equilibrium yielded the *Z*-isomer **20** as the sole product. These results are consistent with the aldolization of the $\beta$,$\beta$-dimethyl aldehyde **3** and ester **1** mentioned earlier, and the reactivity and selectivity of the extended dienolates are under similar control by ATPH. However, as implied by the structural characteristics of the ATPH−**2** complex, we obtained an undesirable product distribution that reflects the distinctive selective coordination of the ketone complex. Both the $\gamma$-methyl and the $\gamma$-methylene of (*E*)-**14** were deprotonated, providing the two different *E*-products **18** and **19**. This suggests that the aldolization step follows formation of the aldehyde, but the preceding deprotonation is the original reaction course of the ketone complex ATPH−(*E*)-**14**.

The corresponding *Z*-isomers (*Z*)-**13**−**15** were subjected to similar transformations (Scheme 2). The reactions of the *Z*-aldehyde **13** and ester **15** were in line with the general selectivity rule seen with the corresponding *E*-isomers. In contrast, the *Z*-ketone **14** again yielded a diversity of products. The $\gamma$-deprotonation−aldolization sequence proceeded exclusively at the $\gamma$-methyl group. This chemoselectivity is similar to that of *Z*-ester **15** rather than *Z*-aldehyde **13**; however, the ensuing aldolization could not control the reactivity of the *s-cis* and *s-trans* conformers of the extended dienolate and gave a mixture of *E*- and *Z*-isomers **19** and **21** as the only isolatable products, the latter being the major isomer. Alcohol **19** was the common product that was produced by both reactions involving (*E*)- and (*Z*)-**14**.

To summarize, each reaction course followed by aldehyde **13**, ester **15**, and ketone **14**, and some supporting experiments are provided.

**Aldehydes.** (*E*)-$\gamma$-Methylene-selective aldolization predominated with (*E*)-**13** to give (*E*)-product **16**, whereas the (*E*)-$\gamma$-methyl of (*Z*)-**13** was alkylated exclusively to give (*E*)-product **17** (Schemes 1 and 2). These experiments emphasize that the (*Z*)-$\gamma$ positions are influenced significantly by the congested environment created by the cavity of ATPH, because the approach of not only electrophiles but also of LDA was circumvented. To confirm the influence of ATPH on the dienolate equilibria, deprotonation of the ATPH−(*E*)-**13** or

***Scheme 1***

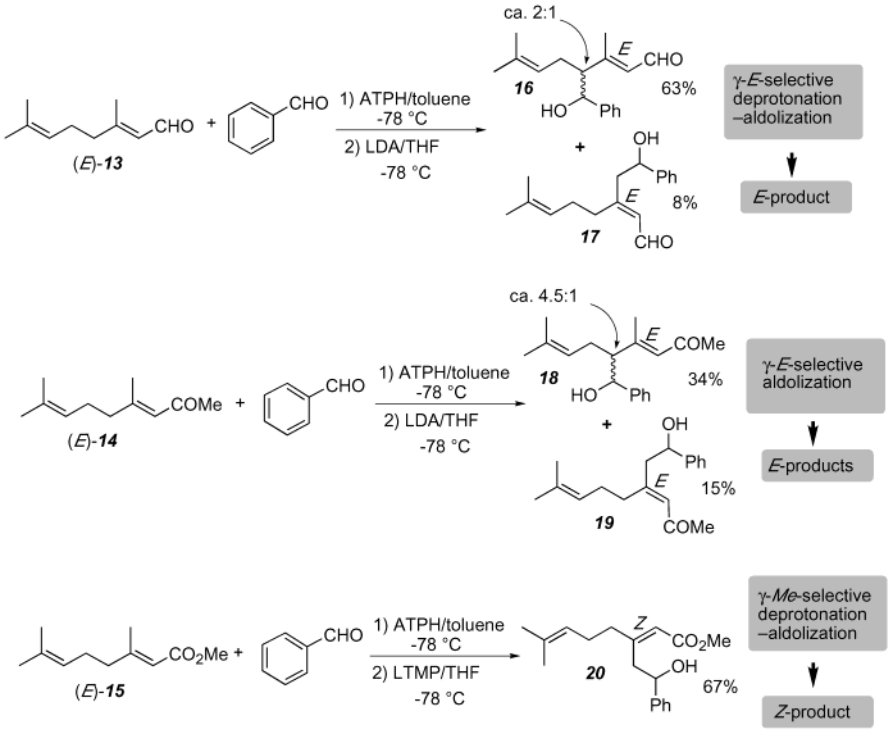

***Scheme 2***

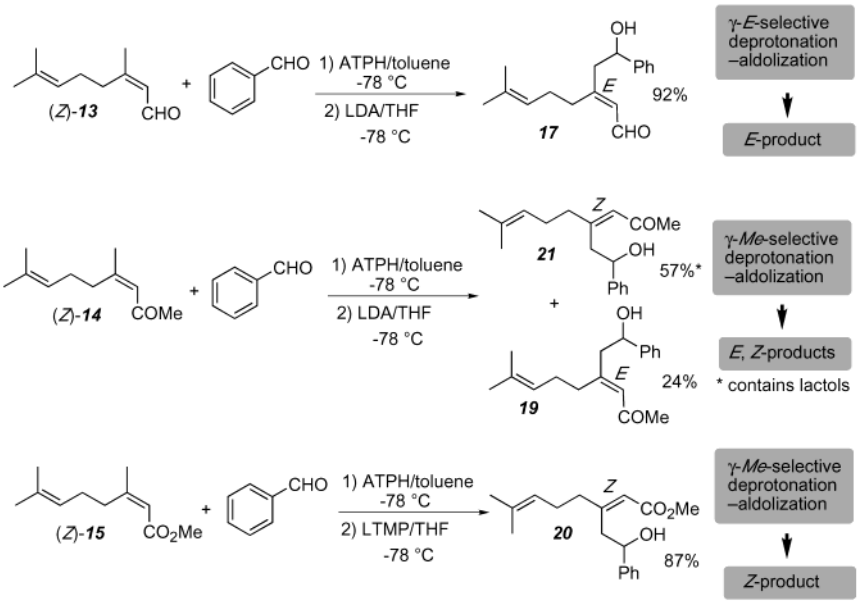


ATPH−(*Z*)-**13** complex with LDA was followed by immediate workup (after ca. 15 s) with excess MeOH at −78 °C. The original *E*/*Z* ratios of (*E*)-**13** (*E*:*Z* = >99:1) and (*Z*)-**13** (*E*:*Z* = <3:97) were partially preserved to give *E*/*Z* ratios of 80:20 and 19:81, respectively, suggesting that the equilibrium shifted to $\mathbf{I_8}$ and $\mathbf{I_9}$ (Figure 11). These results point out that both (*E*)- and (*Z*)-aldehydes **5** must be encapsulated effectively in an *anti*, *s-trans* coordination similar to that of the ATPH−**3** complex.

**Esters.** *E*- and *Z*-acid esters **15** showed γ-methyl-selective deprotonation−aldolization regardless of the original olefin configurations of the esters to give identical (*Z*)-product **20** (Schemes 1 and 2). These results are in agreement with the selective coordination of the ATPH−**1** complex and fast equilibrium between the dienolate conformers $\mathbf{I_{10}}$ and $\mathbf{I_{11}}$. In fact, similar workup experiments with the extended dienolates derived from ATPH−(*E*)-**15** and ATPH−(*Z*)-**15** both resulted in the regeneration of (*E*)-**15** and (*Z*)-**15** in a ratio of ∼80:20. This implies that *s-cis* conformer $\mathbf{I_{10}}$ predominates in a rapid equilibrium and is more reactive with an electrophile. In this case, the predominant dienolate conformer and a more reactive form are identical. The dienolate adopts the *s-cis* form $\mathbf{I_{10}}$ preferentially as it orients the longer, more sterically hindered

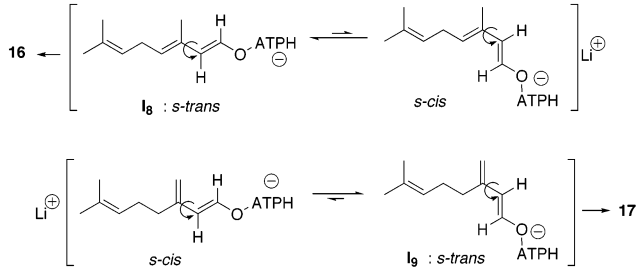


***Figure 11.*** Most important conformational equilibria of extended dienoates.

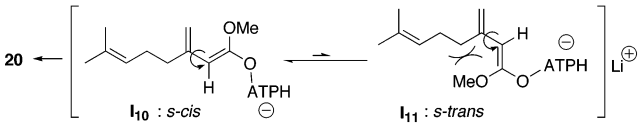


***Figure 12.*** Most important conformational equilibria of extended dienoates.

β-chain into a less congested space. This obviates undesired steric repulsion with the MeO-group of the ester, rather than the steric constraints with ATPH (Figure 12). Thus, the influence of ATPH on the ester is not as large as that on the aldehyde. The observed kinetic attack of LDA or LTMP, which prefers chemoselective deprotonation of a methyl over methylene, also demonstrates that ATPH has negligible steric influence on the ester deprotonation steps. Indeed, the cavity can no longer maintain its original propellerlike structure (Figure 3) due to the selective coordination of esters with relatively small θ (Table 2).

**Ketones.** The distinctive selective coordination of ketones, which has an intermediate θ magnitude, should result in a complicated reaction with **14** to give an isomeric mixture of products. We detected an equivocal nature that is partially consistent with the behavior of either aldehyde **13** or ester **15**. The selectivity depends on the stereochemistry (*E* or *Z*) of the starting ketone.

## Conclusion

We have demonstrated that several β,β-disubstituted-α,β-unsaturated carbonyl substrates can be differentiated by complexation with ATPH. The central feature of the carbonyl recognition event involves selective coordination. Distinctive selective coordination was confirmed by the single-crystal X-ray structures of each ATPH−carbonyl complex, which provided insight into the structure of the corresponding dienolates but also into the structure of the aldol adducts. ATPH was shown to play a prominent role in controlling the reaction of dienolates to give different aldol products, depending on the α,β-unsaturated carbonyl compounds. Thus, we achieved diverse selectivity and reactivity through a set of reactions that involved control of (1) *syn*- versus *anti*-complexation; (2) *s-cis* versus

(26) *Stereochemistry of Organic Compounds*; Eliel, E. L., Wilen, S. H., Eds.; John Wiley & Sons: New York, 1994; Chapter 10.2, p 621. It was suggested that either an *s-cis* or a gauche conformer of butadiene is 1.5−2.6 kcal/mol above the *s-trans* with a barrier to conformational inversion of 5.5−7.3 kcal/mol. Some other data also show the *s-cis* lying ca. 2.9 kcal/mol above the *s-trans* with a rotational barrier from the *s-trans* side of ca. 6.8 kcal/mol.

*s-trans* conformation of carbonyl compounds; (3) the deprotonation site; (4) *s-cis* versus *s-trans* conformation of extended dienolates; and (5) the alkylation site.

## Experimental Section

**General.** Infrared (IR) spectra were recorded on a Shimadzu FTIR-8100 spectrometer. $^1$H NMR spectra were measured on a Varian Gemini-300 spectrometer (300 MHz) at ambient temperature. Data were recorded as follows: chemical shift in ppm from internal tetramethylsilane on the $\delta$ scale, multiplicity (b = broad, s = singlet, d = doublet, t = triplet, and m = multiplet), coupling constant (Hz), integration, and assignment. $^{13}$C NMR spectra were recorded on a Varian Gemini-300 (75 MHz) spectrometer. Chemical shifts were recorded in ppm from the solvent resonance employed as the internal standard (deuterochloroform at 77.07 ppm). All experiments were carried out under an atmosphere of dry argon. For thin-layer chromatography (TLC) analysis throughout this work, Merck precoated TLC plates (silica gel 60 GF254 0.25 mm) were used. The products were purified by preparative column chromatography on silica gel (E. Merck Art. 9385). Microanalyses were conducted at the Faculty of Agriculture, Nagoya University.

In experiments that required dry solvent toluene, toluene-$d_8$, $CH_2Cl_2$, and $CD_2Cl_2$ were freshly distilled from calcium hydride, and tetrahydrofuran (THF) was freshly distilled from sodium metal using benzophenone ketyl as indicator. Organic substrates **1**, **3**, **4**, and **6** were commercially available and were used after distillation. A mixture of ketones **2** and **5** was available from Wako, each being used after separating by column chromatography. *n*-BuLi (hexane solution) was obtained from Mitsuwa. Aldehydes **9a**,[27] **12**,[28] and (*E*)- and (*Z*)-**13**[29] as well as esters **10**[30] and (*E*)- and (*Z*)-**15**[31] are all known compounds, and the former two were prepared by oxidation of geraniol (Wako) and nerol (Wako) over $MnO_2$, respectively. The latter two were prepared by methylation ($BF_4OMe_3$, *i*-$Pr_2NEt$; room temperature, 4 h) of an *E* and *Z* mixture of geranic acid (Aldrich), followed by separation of the resulting methyl ester isomers by column chromatography on silica gel. Ketones (*E*)- and (*Z*)-**14**[32] are also known compounds.

**Preparation of ATPH.** To a solution of 2,6-diphenylphenol (3.0 equiv) in toluene was added at room temperature a 1.0 M hexane solution of $Me_3Al$ (1.0 equiv). Methane gas (~3.0 equiv) evolved immediately. The resulting pale-yellow solution was stirred at room temperature for 0.5 h and used without further purification.

**Typical Procedure for the Regio- and Stereoselective Synthesis of α,β-Unsaturated Carbonyl Compounds Using the Coupling of Two Different Carbonyl Substrates Complexed with ATPH.** The following procedure for the reaction of 3-methyl-2-butenoate (**1**) with benzaldehyde (PhCHO) is representative. To a solution of ATPH (1.65 mmol) in toluene (5.0 mL) were added **1** (131 μL, 1.0 mmol) and PhCHO (51 μL, 0.50 mmol) at −78 °C under argon. After 5 min, LTMP, generated by treatment of a THF (5.0 mL) solution of 2,2,6,6-tetramethylpiperidine (194 μL, 1.1 mmol) with a 1.60 M hexane solution of *n*-BuLi (0.72 mL, 1.1 mmol) at −78 °C for 30 min, was transferred by a cannula to the toluene solution of the mixture of ATPH−**1** and ATPH−PhCHO complexes at −78 °C within ca. 2−3 min. The reaction mixture was stirred at this temperature for 30 min, quenched with aqueous $NH_4Cl$, filtered through a pad of Celite, and extracted with diethyl ether. The organic layer was dried over $Na_2SO_4$ and concentrated. The residue was purified by column chromatography on silica gel (diethyl ether/hexane = 1/3 to 1/4 as the eluent) to give (*Z*)- and (*E*)-**7a** (101 mg, yield 91%) in a ratio of 13:1 as a colorless liquid. 2,6-Diphenylphenol could be recovered in more than 90% isolated yield. In all experiments where α,β-unsaturated aldehydes and ketones were employed, the above procedure was followed, except that ATPH (2.2 equiv), LDA (1.2 equiv), $R^1CHO$ (1.0 equiv), and α,β-unsaturated carbonyl compound (1.0 equiv) were used.

**Methyl (*Z*)-5-Hydroxy-3-methyl-5-phenyl-2-pentenoate ((*Z*)-7a).** IR (neat): 3441, 1714, 1645, 1435, 1174 cm$^{-1}$. $^1$H NMR (300 MHz, $CDCl_3$): $\delta$ 7.46−7.24 (m, 5H), 5.90 (s, 1H), 4.91 (ddd, 1H, $J$ = 3.7, 5.5, 9.6 Hz), 3.90 (d, 1H, $J$ = 5.5 Hz), 3.73 (s, 3H), 3.25 (dd, 1H, $J$ = 9.6, 12.8 Hz), 2.66 (dd, 1H, $J$ = 3.7, 12.8 Hz), 1.91 (s, 3H). $^{13}$C NMR (75 MHz, $CDCl_3$): $\delta$ 168.4, 157.2, 144.8, 128.2 (two peaks are overlapped), 127.2, 118.2, 73.0, 51.3, 43.7, 26.0. Anal. Calcd for $C_{13}H_{16}O_3$: C, 70.89; H, 7.32. Found: C, 70.67; H, 7.48. **((*E*)-7a)** $^1$H NMR (300 MHz, $CDCl_3$): $\delta$ 7.40−7.22 (m, 5H), 5.78 (s, 1H), 4.89 (dd, 1H, $J$ = 4.8, 8.7 Hz), 3.69 (s, 3H), 2.60 (dd, 1H, $J$ = 8.7, 13.8 Hz), 2.51 (dd, 1H, $J$ = 5.2, 14.0 Hz), 2.23 (s, 3H).

**Methyl (*Z*)-5-Cyclohexyl-5-hydroxy-3-methyl-2-pentenoate ((*Z*)-7b).** IR (KBr): 3306, 2920, 1715, 1705, 1646, 1443, 1252, 1198 cm$^{-1}$. $^1$H NMR (300 MHz, $CDCl_3$): $\delta$ 5.84 (d, 1H, $J$ = 1.5 Hz), 3.69 (s, 3H), 3.52 (dtt, 1H, $J$ = 2.7, 7.5, 12.3 Hz), 3.13 (dd, 1H, $J$ = 10.8, 12.6 Hz), 2.97 (d, 1H, $J$ = 6.9 Hz, OH), 2.25 (dd, 1H, $J$ = 2.9, 10.8 Hz), 1.95 (d, 3H, $J$ = 1.5 Hz), 1.94−1.63 (m, 5H), 1.48−0.99 (m, 6H). $^{13}$C NMR (75 MHz, $CDCl_3$): $\delta$ 168.5, 158.7, 117.7, 74.7, 51.2, 45.0, 38.2, 28.9, 27.7, 26.5, 26.27, 26.15, 25.7. Anal. Calcd for $C_{13}H_{22}O_3$: C, 68.99; H, 9.80. Found: C, 68.99; H, 9.89.

**Methyl (*E*)-5-Cyclohexyl-5-hydroxy-3-methyl-2-pentenoate ((*E*)-7b).** IR (neat): 3450, 2926, 1718, 1705, 1647, 1226, 1151 cm$^{-1}$. $^1$H NMR (300 MHz, $CDCl_3$): $\delta$ 5.76 (s, 1H), 3.69 (s, 3H), 3.64−3.50 (m, 1H), 2.37 (dd, 1H, $J$ = 2.1, 13.8 Hz), 2.20 (s, 3H), 2.17 (dd, 1H, $J$ = 9.6, 13.6 Hz), 1.83−1.54 (m, 5H), 1.42−0.98 (m, 7H). $^{13}$C NMR (75 MHz, $CDCl_3$): $\delta$ 166.8, 157.5, 117.6, 73.3, 50.9, 45.8, 43.7, 29.1, 27.8, 26.4, 26.2, 26.1, 18.9. Anal. Calcd for $C_{13}H_{22}O_3$: C, 68.99; H, 9.80. Found: C, 68.98; H, 9.78.

**(*E*)-6-Hydroxy-4-methyl-6-phenyl-3-hexene-2-one ((*E*)-8a).** IR (neat): 3642, 1684, 1613, 1360, 1217, 1057, 968 cm$^{-1}$. $^1$H NMR (300 MHz, $CDCl_3$): $\delta$ 7.32 (m, 5H), 6.08 (s, 1H), 4.87 (m, 1H), 2.54 (m, 1H), 2.45 (dd, 1H, $J$ = 5.1, 8.4 Hz), 2.15 (s, 3H), 2.12 (s, 1H). $^{13}$C NMR (75 MHz, $CDCl_3$): $\delta$ 198.9, 154.1, 143.7, 128.4, 127.7, 126.1, 125.6, 72.0, 50.9, 31.7, 19.3 Anal. Calcd for $C_{13}H_{16}O_2$: C, 76.44; H, 7.90. Found: C, 76.23; H, 8.10.

**(*E*)-6-Hydroxy-4-methyl-6-cyclohexyl-3-hexene-2-one ((*E*)-8b).** IR (neat): 2926, 2858, 1684, 1615, 1451, 1356, 1219 cm$^{-1}$. $^1$H NMR (300 MHz, $CDCl_3$): $\delta$ 6.15 (s, 1H), 3.59 (tt, 1H, $J$ = 3.2, 9.6 Hz), 2.19 (s, 3H), 2.16 (d, 3H, $J$ = 0.6 Hz), 2.11 (ss, 1H, $J$ = 0.6, 9.6 Hz), 1.85−1.60 (m, 5H), 1.42−0.99 (m, 6H). $^{13}$C NMR (75 MHz, $CDCl_3$): $\delta$ 198.6, 155.7, 125.8, 73.3, 46.1, 43.8, 31.8, 29.1, 27.8, 26.4, 26.2, 26.1, 19.3. Anal. Calcd for $C_{13}H_{22}O_2$: C, 74.24; H, 10.54. Found: C, 74.08; H, 10.81.

**(*E*)-5-Cyclohexyl-5-hydroxy-3-methyl-2-pentenal ((*E*)-9b).** IR (neat): 3568, 2856, 1686, 1609, 1211, 1062 cm$^{-1}$. $^1$H NMR (300 MHz, $CDCl_3$): $\delta$ 5.94 (dd, 1H, $J$ = 0.9, 8.1 Hz), 3.67−3.56 (m, 1H), 2.42 (dd, 1H, $J$ = 2.8, 14.1 Hz), 2.26 (dd, 1H, $J$ = 9.6, 13.5 Hz), 2.22 (s, 3H), 1.95−1.55 (m, 6H), 1.45−0.96 (m, 6H). $^{13}$C NMR (75 MHz, $CDCl_3$): $\delta$ 191.0, 162.0, 129.1, 73.7, 45.4, 43.9, 29.1, 27.7, 26.3, 26.1, 26.0, 17.9. Anal. Calcd for $C_{12}H_{20}O_2$: C, 73.43; H, 10.27. Found: C, 73.44; H, 10.48.

**6-Hydroxy-6-phenyl-3-hexene-2-one (11).** IR (neat): 3641, 1698, 1653, 1624, 1364, 1260, 978, 702 cm$^{-1}$. $^1$H NMR (300 MHz, $CDCl_3$): $\delta$ 7.36 (m, 5H), 6.80 (dt, 1H, $J$ = 7.2, 15.9 Hz), 6.10 (d, 1H, $J$ = 15.9 Hz), 4.83 (m, 1H), 2.63 (m, 2H), 2.21 (s, 1H). $^{13}$C NMR (75 MHz, $CDCl_3$): $\delta$ 198.7, 144.0, 143.4, 133.4, 128.6, 127.9, 125.6, 73.0, 42.0, 26.8. Anal. Calcd for $C_{12}H_{14}O_2$: C, 75.76; H, 7.42. Found: C, 75.88; H, 7.51.

**(*E*)-4-(1-Hydroxy-1-phenyl)methyl-3,7-dimethyl-2,6-octadienal (16).** IR (neat): 3427, 2916, 1670, 1454, 1024 cm$^{-1}$. $^1$H NMR (300 MHz,

(27) Duhamel, P.; Cahard, D.; Poirier, J.-M. *J. Chem. Soc., Perkin Trans. 1* **1993**, 2509. See also the Supporting Information of *J. Am. Chem. Soc.* **1998**, *120*, 813.
(28) Bellassoued, M.; Salemkour, M. *Tetrahedron* **1996**, *52*, 4607.
(29) Compared directly with commercially available samples. Also see: Bobbitt, J. M. *J. Org. Chem.* **1998**, *63*, 9367.
(30) Dugger, R. W.; Heathcock, C. H. *J. Org. Chem.* **1980**, *45*, 1181.
(31) Burrel, J. W.; Garwood, R.; Jackman, L. M.; Oskay, E.; Weedon, B. C. *J. Chem. Soc. C* **1966**, 2145.
(32) Yoshioka, M.; Ishii, K.; Wolf, H. R. *Helv. Chim. Acta* **1980**, *63*, 571.

$CDCl_3$): δ 10.0 (d, 1H, $J$ = 9.0 Hz), 7.40−7.26 (m, 5H), 5.97 (d, 1H, $J$ = 7.9 Hz), 4.86 (t, 1H, $J$ = 7.1 Hz), 4.66 (d, 1H, $J$ = 8.8 Hz), 2.56−2.47 (m, 1H), 2.17 (s, 3H), 2.10−1.87 (m, 2H), 1.60 (s, 3H), 1.41 (s, 3H). $^{13}$C NMR (75 MHz, $CDCl_3$): δ 191.0, 164.0, 142.4, 133.5, 130.0, 128.5 (two peaks are overlapped), 128.1, 126.6 (two peaks are overlapped), 120.6, 76.0, 57.7, 28.5, 25.6, 17.7, 15.6. Anal. Calcd for $C_{17}H_{22}O_2$: C, 79.03; H, 8.58. Found: C, 78.99; H, 8.83.

**(*E*)-3-(2-Hydroxy-2-phenyl)ethyl-7-methyl-2,6-octadienal (17).** IR (neat): 3429, 2968, 1666, 1450, 1051 cm$^{-1}$. $^1$H NMR (300 MHz, $CDCl_3$): δ 9.91 (d, 1H, $J$ = 8.1 Hz), 7.40−7.27 (m, 5H), 5.96 (d, 1H, $J$ = 8.0 Hz), 5.09 (t, 1H, $J$ = 7.4 Hz), 4.91 (dd, 1H, $J$ = 5.2, 8.0 Hz), 2.72−2.48 (m, 4H), 2.27−2.19 (m, 2H), 2.09 (bs, 1H), 1.67 (s, 3H), 1.57 (s, 3H). $^{13}$C NMR (75 MHz, $CDCl_3$): δ 190.9, 163.6, 143.7, 133.7, 129.6, 128.5 (two peaks are overlapped), 127.8, 125.6 (two peaks are overlapped), 122.1, 72.6, 47.3, 31.4, 27.3, 25.5, 17.7. Anal. Calcd for $C_{17}H_{22}O_2$: C, 79.03; H, 8.58. Found: C, 78.94; H, 8.76.

**4,8-Dimethyl-6-(1-methyl-1-phenylmethyl)-(3*E*)-3,7-nonadien-2-one (18: More Polar).** IR (neat): 2965, 1686, 1676, 169, 1453, 1377, 1354, 700 cm$^{-1}$. $^1$H NMR (300 MHz, $CDCl_3$): δ 7.37−7.30 (m, 5H), 6.16 (s, 1H), 4.83 (t, 1H, $J$ = 7.3 Hz), 4.62 (d, 1H, $J$ = 8.7 Hz), 2.42−2.34 (m, 1H), 2.20 (s, 3H), 2.15 (d, 3H, $J$ = 1.2 Hz), 2.07−1.96 (m, 1H), 1.85−1.78 (m, 1H), 1.59 (s, 3H), 1.41 (s, 3H). $^{13}$C NMR (75 MHz, $CDCl_3$): δ 198.4, 157.6, 142.4, 133.1, 128.5, 128.1, 127.1, 126.9, 121.0, 75.7, 58.4, 32.0, 28.1, 25.6, 17.7, 16.1. Anal. Calcd for $C_{19}H_{24}O_2$: C, 79.37; H, 8.88. Found: C, 79.29; H, 9.04. **(18: less polar)** IR (neat): 2965, 1682, 1615, 1609, 1456, 1356, 1211, 764, 702 cm$^{-1}$. $^1$H NMR (300 MHz, $CDCl_3$): δ 7.33−7.23 (m, 5H), 5.86 (s, 1H), 4.99 (m, 1H), 4.69 (d, 1H, $J$ = 7.2 Hz), 2.58−2.52 (m, 1H), 2.47−2.40 (m, 1H), 2.32−2.21 (m, 1H), 2.02 (s, 3H), 1.96 (s, 3H), 2.65 (s, 3H), 1.59 (s, 3H). $^{13}$C NMR (75 MHz, $CDCl_3$): δ 198.5, 157.1, 142.7, 133.1, 128.2, 127.7, 126.3, 126.2, 121.7, 77.5, 76.4, 58.0, 31.8, 27.5, 25.7, 18.1, 17.9. Anal. Calcd for $C_{19}H_{24}O_2$: C, 79.37; H, 8.88. Found: C, 79.18; H, 9.14.

**8-Methyl-4-(2-methyl-2-phenylethyl)-(3*E*)-3-nonadien-2-one (19).** IR (neat): 2926, 2853, 1671, 1449, 1200, 1124 cm$^{-1}$. $^1$H NMR (300 MHz, $CDCl_3$): δ 7.36−7.27 (m, 5H), 6.10 (s, 1H), 5.15 (tt, 1H, $J$ = 1.5, 7.5 Hz), 4.86 (dd, 1H, $J$ = 5.5, 7.7 Hz), 2.56−2.41 (m, 3H), 2.17−2.14 (m, 2H), 2.15 (s, 3H), 1.68 (s, 3H), 1.63 (s, 3H). $^{13}$C NMR (75 MHz, $CDCl_3$): δ 198.2, 157.8, 143.7, 132.4, 128.5, 127.8, 126.2, 125.7, 123.5, 72.3, 48.6, 32.4, 31.8, 27.0, 25.7, 17.6. Anal. Calcd for $C_{19}H_{24}O_2$: C, 79.37; H, 8.88. Found: C, 79.13; H, 9.08.

**Methyl 3-(2-Hydroxy-2-phenyl)ethyl-7-methyl-(2*Z*)-2,6-octadienoate (20).** IR (neat): 3441, 2928, 1695, 1641, 1435 cm$^{-1}$. $^1$H NMR (300 MHz, $CDCl_3$): δ 7.46−7.24 (m, 5H), 5.89 (s, 1H), 5.08−5.04 (m, 1H), 4.92−4.86 (m, 1H), 4.00 (d, 1H, $J$ = 5.9 Hz, −OH), 3.75 (s, 3H), 3.24 (dd, 1H, $J$ = 9.9, 12.9 Hz), 2.64 (dd, 1H, $J$ = 3.5, 12.9 Hz), 2.18 (bs, 4H), 1.69 (s, 3H), 1.59 (s, 3H). $^{13}$C NMR (75 MHz, $CDCl_3$): δ 168.6, 160.7, 145.1, 132.6, 128.3 (two peaks are overlapped), 127.2, 125.4 (two peaks are overlapped), 122.7, 117.5, 73.4, 51.4, 42.6, 38.7, 26.0, 25.6, 17.7. Anal. Calcd for $C_{18}H_{24}O_3$: C, 74.97; H, 8.39. Found: C, 74.84; H, 8.22.

**8-Methyl-4-(2-methyl-2-phenylethyl)-(3*Z*)-3,7-nonadien-2-one (21: Keto Alcohol).** 7.45−7.25 (m, 5H), 6.31 (s, 1H), 5.15 (m, 1H), 4.88−4.82 (m, 2H), 3.07 (dd, 1H, $J$ = 9.6, 12.6 Hz), 2.56 (dd, 1H, $J$ = 3.3, 12.6 Hz), 2.29−2.10 (m, 4H), 2.25 (s, 3H), 1.69 (s, 3H), 1.61 (s, 3H). $^{13}$C NMR (75 MHz, $CDCl_3$): δ 201.1, 158.7, 142.1, 139.3, 132.1, 128.4, 94.8, 73.3, 70.3, 43.3, 38.7, 36.6, 36.0, 31.0, 29.5, 26.1, 25.74, 25.68, 17.7. These peaks are those corresponding to the keto alcohol and lactol forms, which were unable to be fully assigned. The initially formed keto alcohol gradually decomposed to the lactol by standing at room temperature. Anal. Calcd for $C_{19}H_{24}O_2$: C, 79.37; H, 8.88. Found: C, 79.20; H, 9.10. **(21: lactol)** IR (neat): 3566, 2916, 1674, 1606, 1456, 1375, 1201 cm$^{-1}$. $^1$H NMR (300 MHz, $CDCl_3$): δ 7.45−7.25 (m, 5H), 5.57 (d, 1H, $J$ = 1.2 Hz), 5.14−5.05 (m, 1H), 5.01 (dd, 1H, $J$ = 3.6, 11.1 Hz), 2.49 (s, 1H), 2.20−2.02 (m, 6H), 1.69 (s, 3H), 1.61 (s, 3H), 1.57 (s, 3H).

The structures assigned to **16**, **17**, and **20** were rigorously established by NOSEY and DEPT measurement. The (*Z*)-structure of **20** was further assigned by conversion to the corresponding δ-lactone as depicted below.

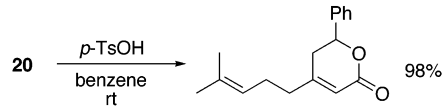


**NMR Experiments. NOE Enhancement Measurement Using the ATPH−1, ATPH−2, ATPH−3, and ATPH−4 Complexes.** To a toluene-$d_8$ solution of 2,6-diphenylphenol (3.0 equiv) was added a toluene-$d_8$ solution (1.0 M) of $Me_3Al$ (1.0 equiv) at room temperature under argon atmosphere. After being stirred for 0.5 h, to the resulting solution of ATPH was added **1** (1.0 equiv) (or **2**−**4** (1.0 equiv)), and each ATPH complex was transferred by a gastight syringe into a NMR sampling tube, which had been degassed and into which argon gas had been substituted. The $^1$H NMR peak assignment of (*E*)- and (*Z*)-γ-methyl groups of the ATPH−**1**, −**2**, −**3**, and ATPH−**4** complexes was performed by measuring NOE enhancement between $H_a$ and $H_d$, and that between $H_b$ and $H_c$ as follows.

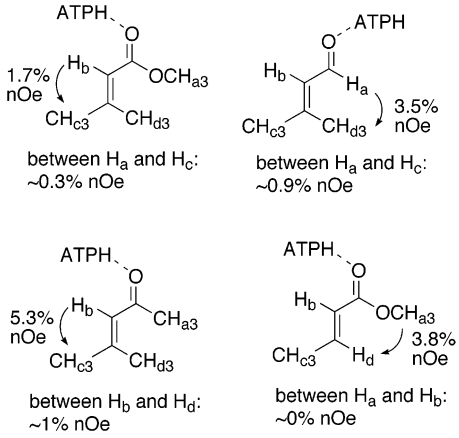


**NOE Enhancement Measurement of the Extended Dienolates Generated by Treatment of a Lithium Amide with the ATPH−1, −2, −3, and −4 Complexes.** Following a procedure similar to that above, ATPH in deuterated solvents was prepared at room temperature, cooled to −78 °C, and **1** (or **2**−**4**) was added. A THF-$d_8$ solution of lithium amide was prepared as follows. To a solution of a secondary amine (*i*-$Pr_2NH$ for ATPH−**2** and −**3** or 2,2,6,6-tetramethylpiperidine for ATPH−**1** and −**4**) (0.33 mmol) in dry THF (3.0 mL) was added a 1.60 M hexane solution of *n*-BuLi at 0 °C under argon atmosphere, and the mixture was stirred for 30 min. Solvents were evaporated in vacuo ($1.0 \times 10^{-3}$ Torr) at this temperature under extremely anhydrous and anaerobic conditions using a Schlenk line. Argon gas (purity: 99.99%), passed sequentially through deoxygenation and dehydration columns, was purged into the flask containing the resulting solidic lithium amide, and dry THF-$d_8$ (6.0 mL) was added. After being cooled to −78 °C, this lithium amide solution was transferred by a steel cannula into the above-prepared and precooled solution of the ATPH−carbonyl complex. The mixture was stirred at −78 °C for 5 min. The resulting solution of the extended dienolate was transferred using a cannula into a NMR sampling tube which had been filled with argon and subsequently cooled to −195.8 °C using a liquid $N_2$ bath. After a couple of minutes, the mixture in the tube solidified in the cooling bath (−195.8 °C), and at this moment the tube was immersed in a MeOH−dry ice bath (−78 °C). After everything was thawed and had become solution, the sample was subjected to a low-temperature NMR measurement at −78 °C.

**Preparation of Single Crystals of ATPH−Carbonyl Complexes for X-ray Diffraction Analysis. The ATPH−1 Complex.** To a solution of ATPH (0.5 mmol) in $CH_2Cl_2$ (4.0 mL)−hexane (0.5 mL) was added ester **1** (0.5 mmol) at room temperature under argon atmosphere. After 30 min, treatment with hexane (5.0 mL) resulted in precipitation of colorless crops, followed by slow addition of $CH_2Cl_2$ (2.0 mL), during which time heating was continued until redissolution of the crops was completed. The mixture was allowed to stand at room temperature for 1−2 days with rigorous exclusion of air and moisture to give colorless (or pale-yellow) crystals.

**The ATPH−2 Complex.** To a solution of ATPH (0.5 mmol) in $CH_2Cl_2$ (2.0 mL) was added mesityloxide (**2**) (0.5 mmol) at room temperature under argon atmosphere. The stirring was stopped after 5 min. To this mixture was added hexane (2.0 mL). The mixture was allowed to stand at room temperature for 1−2 days with rigorous exclusion of air and moisture to give bright yellow crystals.

**The ATPH−3 Complex.** To a solution of ATPH (0.5 mmol) in $CH_2Cl_2$ (4.0 mL)−hexane (0.5 mL) was added aldehyde **3** (0.5 mmol) at room temperature under argon atmosphere. After 30 min, the addition of hexane (2.0 mL) resulted in precipitation of yellow-orange crops, which were subsequently entirely redissolved by heating. The mixture was allowed to stand at room temperature for 1−2 days with rigorous exclusion of air and moisture to give orange crystals.

**The ATPH−4 Complex.** To a solution of ATPH (0.5 mmol) in $CH_2Cl_2$ (2.0 mL) was added ester **4** (0.5 mmol) at room temperature under argon atmosphere. After 30 min, the addition of hexane (5.0 mL) resulted in precipitation of pale-yellow crops, which were subsequently entirely redissolved by heating, during which time $CH_2Cl_2$ was added. The mixture was allowed to stand at room temperature for 1−2 days with rigorous exclusion of air and moisture to give colorless (or pale-yellow) crystals.

**The ATPH−6 Complex.** To a solution of ATPH (0.5 mmol) in $CH_2Cl_2$ (4.0 mL) was added crotonaldehyde **6** (0.5 mmol) at room temperature under argon atmosphere. After 30 min, the addition of hexane (1.4−1.6 mL) resulted in precipitation of yellow-orange crops, which were subsequently entirely redissolved by heating. The mixture was allowed to stand at room temperature for 1−2 days with rigorous exclusion of air and moisture to give orange crystals.

**X-ray Crystallographic Determinations.** Each single crystal of the ATPH−**1**, −**2**, −**3**, −**4**, and ATPH−**6** complexes suitable for X-ray diffraction analysis was transferred to a glass capillary tube as quickly as possible under air atmosphere, and the glass capillary was mounted with a sticky compound on a goniometer for measurement. Diffraction data were obtained with graphite-monochromated Mo Kα radiation on a MAC Science DIP2030 diffractometer. Standard reflections for each data set showed no significant decrease in intensity throughout acquisition. All non-hydrogen atoms were located from the direct method, where the full-matrix was used for least-squares data. All non-hydrogen atoms were refined anisotropically. The hydrogens of all of the methyl groups were refined from an initial idealized position (0.96 Å), and the other hydrogens were found by Fourier synthesis, using isotropic temperature factors. Crystallographic computations were performed on a Silicon Graphics INDY computer using the maXus program for data reduction, determining the structure, refining the structure, and molecular graphics. MAC DENZO software was used for cell refinement.

**Acknowledgment.** We are grateful to Ms. Akiko Nakao (MacScience Co., Ltd.) for her helpful suggestions on solving the crystal structures of ATPH complexes.

**Supporting Information Available:** X-ray crystallographic files for crystal structures of ATPH−**1**, −**2**, −**3**, −**4**, and −**6** (PDF). This material is available free of charge via the Internet at http://pubs.acs.org.

JA0205941